Published in final edited form as:
Neurobiol Dis. 2012 September ; 47(3): 358–366. doi:10.1016/j.nbd.2012.05.016.

Pyramidal cells accumulate chloride at seizure onset

Kyle P Lillis[a,b], **Mark A Kramer**[c], **Jerome Mertz**[d], **Kevin J Staley**[a,b], and **John A White**[e]

[a]Department of Neurology, Massachusetts General Hospital, 114 16th St #2600, Charlestown, MA 02129, lillis.kyle@mgh.harvard.edu, staley.kevin@mgh.harvard.edu

[b]Harvard Medical School, 25 Shattuck Street, Boston, MA 02115

[c]Department of Mathematics & Statistics, Boston University, 111 Cummington Street, Boston, MA 02215, mak@bu.edu

[d]Department of Biomedical Engineering, Boston University, 44 Cummington Street, Boston, MA 02215, jmertz@bu.edu

[e]Department of Bioengineering, University of Utah, 20 S. 2030 E., Salt Lake City, UT 84112, Phone: 801-587-1200, Fax: 801-585-5151, john.white@utah.edu

Abstract

Seizures are thought to originate from a failure of inhibition to quell hyperactive neural circuits, but the nature of this failure remains unknown. Here we combine high-speed two-photon imaging with electrophysiological recordings to directly evaluate the interaction between populations of interneurons and principal cells during the onset of seizure-like activity in mouse hippocampal slices. Both calcium imaging and dual patch clamp recordings reveal that *in vitro* seizure-like events (SLEs) are preceded by pre-ictal bursts of activity in which interneurons predominate. Corresponding changes in intracellular chloride concentration were observed in pyramidal cells using the chloride indicator Clomeleon. These changes were measurable at SLE onset and became very large during the SLE. Pharmacological manipulation of GABAergic transmission, either by blocking $GABA_A$ receptors or by hyperpolarizing the $GABA_A$ reversal potential, converted SLEs to short interictal-like bursts. Together, our results support a model in which pre-ictal $GABA_A$ receptor-mediated chloride influx shifts E_{GABA} to produce a positive feedback loop that contributes to the initiation of seizure activity.

Keywords

epilepsy; ictogenesis; chloride accumulation; ion imaging; calcium; seizure; GABA; chloride transport; interneuron; targeted path scanning

Introduction

The failure of GABAergic inhibition has long been cited as a contributing factor to the generation of seizures in epilepsy. Pathological changes to inhibitory circuits have been argued to occur through the death of interneurons (de Lanerolle et al., 1989), change in the

Correspondence to: John A White.

organization of GABAergic synapses (Marchionni and Maccaferri, 2009; Thind et al., 2010), or reduction in interneuron excitability (Martin et al., 2010). While epilepsy is clearly associated with changes in the anatomical organization of GABAergic networks, the pathophysiological action of GABA in seizure generation remains unclear (Cossart et al. 2005). In particular, it is difficult to determine whether GABA changes are adaptive or causal solely by examining the anatomical changes that occur in animal models of epilepsy.

Some studies have begun to link dysfunction in GABAergic interneurons to onset of epileptiform activity. For example, when firing at supraphysiological rates, interneurons can also be *transiently* rendered ineffective at inhibiting postsynaptic targets either by entering depolarization block (Ziburkus et al., 2006) or by causing post-synaptic chloride to accumulate to depolarizing concentrations, effectively making $GABA_A$ synapses excitatory (Staley et al., 1995; Taira et al., 1997; Köhling et al., 2000; Fujiwara-Tsukamoto et al., 2004; Ben-Ari and Holmes, 2005). The latter mechanism would have the effect of transforming feedback inhibition into feedback excitation, producing an unstable, positive-feedback network. Large preictal alterations in the reversal potential of synaptic events associated with epileptiform spikes have recently been reported. Although the responsible neurotransmitter was proposed to be glutamate, some interneurons were found to fire prior to the preictal discharges (Huberfeld et al., 2011). Interestingly, reduced expression of the outwardly-directed chloride transporter KCC2 have been found in both experimental (de Guzman et al., 2006) and human epilepsy (Aronica et al., 2007; Shimizu-Okabe et al., 2011; Huberfeld et al., 2011). Electrophysiological assays of KCC2 transport have demonstrated reduced KCC2 transport capacity in multiple experimental models (Jin et al., 2005; Pathak et al., 2007; Lee et al., 2011). These studies support the possibility that the chloride gradient may be selectively labile in chronic epilepsy, and that chloride accumulation may be a pre-ictal mechanism of activity-dependent loss of inhibition.

Due to technical challenges in recording from large neural networks with cellular resolution, studying the physiology of this complex balance between excitation and inhibition in neural circuits has primarily been constrained to pharmacological manipulation and single-cell or paired intracellular recordings (Köhling et al., 2000; Huberfeld et al., 2011). Here, we combine these classic techniques with recently developed network imaging methods (Lillis et al., 2008) to measure the interactions between populations of inhibitory cells and principal cells of the hippocampus and entorhinal cortex. We find that the pre-ictal burst (also called “pre-ictal spike” or “sentinel spike”) is dominated by epileptiform activity in the population of somatostatin-positive GABAergic interneurons. Chloride imaging reveals that this GABAergic hyperactivity leads to a flux of chloride and leaves the population of post-synaptic pyramidal cells in a highly excitable state just before seizure onset. At seizure onset, there is a massive increase in intracellular chloride that is sufficient to make GABA currents excitatory.

Materials and Methods

Acute slice preparation

Acute slice protocols were approved by the Boston University Animal Care and Use Committee. Transverse hippocampal brain slices (400 μm) were prepared as previously described (Netoff et al., 2005) from juvenile (P10-P20) mice expressing GFP in somatostatin-positive interneurons under the control of the Gad1 (GAD67) promoter (strain FVB-Tg(GadGFP)45704Swn/J, Jackson Laboratories, Bar Harbor, ME) or from Clomeleon mice. After a 1hr incubation period, they were transferred to the recording chamber where they were bathed is artificial cerebrospinal fluid (ACSF, in mM, 126 NaCl, 2.5 KCl, 1.25 NaH_2PO_4, 2 $MgCl_2$, 26 $NaHCO_3$, 25 dextrose, 2mM $CaCl_2$). 50μM 4-aminopyridine was added to induce epileptiform activity. In some experiments 10μM acetazolamide was added

inhibit carbonic anhydrase. To elicit seizures in Clomeleon acute slices, which did not spontaneously seize in 50 μM 4-AP, $MgCl_2$ was omitted from the ACSF (in addition to adding 50 μM 4-AP). All chemicals were obtained from Sigma-Aldrich (St. Louis, MO). Slices were initially visualized using oblique illumination.

Organotypic slice culture preparation

Organotypic slice culture protocols were approved by the Massachusetts General Hospital Subcommittee on Research Animal Care. Roller tube type organotypic slice cultures were prepared as described by (Gähwiler, 1981). Briefly, isolated hippocampi from P6–8 CLM-1 mouse pups were cut into 350-μm slices on a McIlwain tissue chopper (Mickle Laboratory Eng. Co., Surrey, United Kingdom). Slices were mounted in clots of chicken plasma (Cocalico Biologicals, Reamstown, PA) and thrombin (Sigma-Aldrich, St. Louis, MO) on poly-l-lysine-(Sigma-Aldrich) coated glass coverslips (Electron Microscopy Sciences, Hatfield, PA) and incubated in roller tubes (Nunc, Roskilde, Denmark) at 5% CO_2, 36°C in 750μL Neurobasal-A growth medium with 2% B27, 500uM Glutamax, and 0.03 mg/mL gentamycin added (all from Invitrogen, Carlsbad, CA). Growth medium was changed every 7 days. Recordings were made in growth media, some with the addition of 10μM GABAzine (SR 95531).

Staining and imaging

Areas of interest were stained with Indo-1 AM (Invitrogen, Carlsbad, CA) using an adapted version of multicell bolus loading (Stosiek et al., 2003; but c.f. Garaschuk et al., 2006), in which a Picospritzer II (Parker Hannifin, Pine Brook, NJ) is used to inject dye through a glass pipette directly into the brain tissue. In this modified version of MCBL, a larger-tip pipette was used (~2MΩ when filled with KCl-based dye solution) to inject many sites for a shorter duration (~5s) than that previously described (1–2min). This resulted in the staining of a large area, with relatively low background staining. The dye used for these experiments, Indo-1, is a ratiometric calcium dye, emitting at a shorter wavelength when bound to calcium. However, the two-photon cross section of calcium-bound Indo-1 is so low that it is essentially invisible when using excitation light longer than 750nm (Xu et al., 1996). We take advantage of this by imaging at 820nm (a wavelength that conveniently excites both GFP and calcium-unbound Indo-1) to get relative calcium measurements with high sensitivity. Because, in this configuration, fluorescence decreases when a cell is active, all Indo-1 fluorescence traces shown have been inverted for clarity.

All images of calcium dynamics were acquired using Targeted Path Scanning (Lillis et al., 2008). All images were acquired using a 20× 0.95 NA water immersion objective (Olympus, Tokyo, Japan). The calcium traces for each cell were then filtered using a 15 point median filter and a 10 point boxcar filter. To average calcium traces taken with different sampling rates (as is inherent to TPS, mean sampling rate for calcium data shown = 51.8Hz), traces were upsampled using the Matlab (The Mathworks, Natick, MA) function *resample*, which interpolates using a polyphase filter. In 4-AP, SLEs occurred approximately once every 4 minutes. To guarantee that a SLE would be captured, a four-minute scan was initiated 2–3 minutes after the previous SLE. I/E ratios were calculated, for each recording, by dividing the mean interneuron calcium trace by the mean principal neuron calcium trace.

Clomeleon images were acquired using custom-designed software and the scanhead from a Radiance 2000MP (BioRad, Hemel Hempstead, UK), equipped with a 20× 0.95 NA water-immersion objective (Olympus, Tokyo, Japan), and PMTs with appropriate filters for YFP (545/30) and CFP (450/80). A SpectraPhysics MaiTai laser (Newport, Irvine, CA), set to 860nm, was used for two-photon excitation. Chloride concentrations were obtained by performing a calibration as previously described (Glykys et al., 2009) using 10μM of the K^+/

H^+ ionophore nigericin, 100μM of OH^-/Cl^- antiporter tributyltin chloride, and known concentrations of extracellular chloride. YFP/CFP ratios for all selected cells were low-pass filtered at 0.5Hz and, because CFP and YFP bleach at different rates (Kuner and Augustine, 2000), a linear trend was subtracted to remove the effect of differential bleaching. For the pre-ictal burst-triggered averaging shown in Figure 3, chloride traces were resampled in the same manner described above for calcium traces. pH changes were measured by staining organotypic slice cultures with SNARF-1-AM by incubating them for >1hr in 10uM dye. Because of the spectral overlap between SNARF-1 and Clomeleon, wild type mice were used for pH imaging experiments. Images were acquired using TPS with an excitation wavelength of 820nm and PMT emission filters centered at 585 and 640. The ratio of light emitted at 585 and 640nm was recorded and linearly detrended (to correct for bleaching) and adjusted to baseline pH using a calibration strategy previously described (Sheldon et al., 2004).

Electrophysiology

During imaging recordings, either a field potential recording (<1MΩ, filled with ACSF or 1M KCl) or a patch-clamp recording (3–6MΩ, filled with 130 mM potassium gluconate, 10mM KCl, 10 mM HEPES, 4 mM Mg-ATP, 0.4 mM Tris-GTP, and 50μM Indo-1 pentapotassium salt) was acquired simultaneously from the region being imaged. For dual-patch clamp recordings, the patch electrodes were targeted to GFP+ and GFP− cells using two-photon imaging. The seal was formed (and ruptured in the case of whole-cell recordings), using oblique illumination for visualization. Whole-cell access was evaluated by monitoring input resistance and imaging the presence of dye in the cell. All electrophysiological recordings were obtained with a Multiclamp 700B, AxoClamp 2B (Axon Instruments, Foster City, CA), or Cornerstone EX4-400 (Dagan, Minneapolis, MN).

Statistical Analyses

For comparison of two populations (e.g. principal cells vs. interneurons), a Kruskal-Wallis analysis was used to test for a significant difference between the two medians. For comparisons to zero (e.g. number of seizures in Figure 5B), a Wilcoxon signed rank test for zero median was performed. For tests of linear correlation, a p-value for Pearson's correlation was computed using Student's t-distribution.

Spike-timing jitter was computed by analyzing the variability in principal neuron spike delay following an interneuron spike for the 10 spikes preceding a pre-ictal burst and the 10 spikes following the pre-ictal burst. Jitter was quantified as the coefficient of variation (CV) or standard deviation (SD) of interneuron->principal neuron spike delay.

Results

Targeted path scanning of inhibition-excitation interplay at seizure onset

In acute slices of hippocampus/entorhinal cortex, 4-aminopyridine (4-AP) initiates seizures that originate in the entorhinal cortex (Avoli et al., 1996; Barbarosie and Avoli, 1997), where interneurons appear (using DIC microscopy) anatomically similar to principal cells. To distinguish interneurons from putative excitatory cells in this region, we prepared slices from mice expressing GFP in 15–35% of somatostatin-positive GAD67-expressing cells (Oliva et al., 2000). Since >92% of neurons in the entorhinal cortex are principal cells (Kumar and Buckmaster, 2006) and 10–20% of all interneurons in these mice express GFP (Oliva et al., 2000), we refer to GFP-negative cells as principal neurons. Actual differences between interneurons and principal neurons might be slightly larger than we measure due to the presence of some interneurons in the GFP-negative population. We used two-photon, calcium imaging combined with targeted path scanning (TPS, Figure 1A, Lillis et al., 2008),

to image epileptiform activity, induced by conditions that leave inhibition intact, in populations of entorhinal cortical interneurons and principal cells.

Seizure-like events, induced by potassium channel blocker, 4-aminopyridine (4-AP) or developing spontaneously in organotypic slice cultures of the hippocampus (Dyhrfjeld-Johnsen et al., 2010), consist of a stereotypical firing pattern (Figure 1B) that begins with a pre-ictal burst, is followed a few seconds later by powerful ictal tonic firing (Figure 1C), then transitions to post-ictal clonic discharges before terminating completely. The data presented here will focus on the preictal burst, which we define as a burst of activity preceding the tonic phase of the seizure by <10s. Using TPS to scan both GFP+ and GFP− cells (i.e. interneurons vs. principal cells) produced calcium traces that could be grouped by cell type and provided sufficient spatial and temporal resolution to analyze the interaction between inhibition and excitation during ictogenesis (Figure 1D).

Interneurons fire at higher rates than principal cells at ictogenesis

TPS recordings revealed that the ratio of interneuron to principal neuron calcium signal (mean interneuron / mean principal neuron, for each recording) significantly increased during pre-ictal bursts (t=0, Figure 1E, n=22 SLEs in slices from 7 animals, each slice with an average of 21 principal cells and 5 interneurons imaged, $p<0.01$). To verify that the proportionally larger calcium transients in interneurons are not a result of differences in calcium buffering capacity, we performed simultaneous patch clamp recordings from interneurons and principal cells. We used both whole-cell patch clamp (Figure 2A) and loose-patch clamp (to avoid dialyzing the cell, Figure 2B) to compare instantaneous firing rates (calculated at each action potential as the inverse of interspike interval) in interneurons and principal cells. We found that, indeed, pre-ictal bursts are dominated by interneuron firing (Figure 2C, 4-AP, n=5 slices from 3 animals, $p< 0.05$). Prior to the pre-ictal burst, interneurons fire apparently randomly with respect to principal cells, with a large coefficient of variation and standard deviation of the intervals between spikes in the two cell types (CV=15.09±12.75, SD = 8.60±6.35 pre-burst). Interestingly, in recordings with action potentials in the seconds following the pre-ictal burst, just before ictogenesis, interneuron and principal cell firing are tightly coupled (CV=0.11±0.04, SD=0.30±0.12 post-burst), with the interneuron leading the principal cell by 4.9±1.7ms (mean±SEM, n=5, 14 spike pairs, Figures 2A,B, insets). However, the sparsity of principal cell firing before the pre-ictal burst make spike jitter difficult to interpret.

To quantify temporal relationships among imaged calcium signals, we performed windowed, cross-correlation-based network analysis. By finding the time lag at which peak correlation occured for all pairs of calcium traces, we were able to determine if each imaged cell was, on average, leading or following activity in the network. We found that, at the time of the pre-ictal burst, interneurons lead activity in the network (Supplemental Figure 1).

GABAergic depolarization contributes to SLE generation

If intense epochs of interneuron firing resulted in chloride influx sufficient to overwhelm the chloride transporter KCC2, then the resultant chloride accumulation should be evident by chloride imaging (Dallwig et al., 1999). We directly tested the hypothesis that chloride accumulates in neurons during SLEs using samples prepared from clomeleon mice (CLM-1), which express a chloride-sensitive ratiometric CFP-YFP construct in a subset of principal neurons and interneurons under control of the Thy1 promoter (Kuner and Augustine, 2000; Berglund et al., 2006). CLM-1 mice are constructed on a C57 background, a strain that is resistant to 4-AP-induced seizures (Kosobud and Crabbe, 1990). To record chloride transients associated with inhibition-intact epileptiform activity, we used chronically epileptic CLM-1 hippocampal organotypic slice cultures, which spontaneously

(without the addition of drugs) produce tonic-clonic seizures similar to those observed in 4-AP-treated acute slices from GIN mice (McBain et al., 1989; Berdichevsky et al., 2009; Dyhrfjeld-Johnsen et al., 2010) and verified results using acute slices from CLM-1 mice treated with 4-AP and zero-Mg^{2+}. Under control conditions, organotypic slice cultures exhibited a mixture of interictal-like and seizure-like activity (13/65 events were longer than 20s, Figure 3A,4C), while in 10μM GABAzine, 184/185 events were less than 5s in duration, with a maximum duration of 5.8s (n=4 slice cultures from two mice, Figure 3B, 4D). Interestingly beginning at the pre-ictal burst, and dramatically accelerating at seizure onset, SLEs (events >20s) produced a sharp decrease in YFP/CFP ratio, corresponding to an increase in chloride of 22.95±0.73mM (mean±SEM, n=4 slice cultures, 13 SLEs, Figure 3A, 4A). For pre-ictal bursts preceding the SLE by >1s, it was possible to isolate a pre-ictal burst-induced chloride transient of 6.27±1.23mM (mean±SEM, Figure 3E, n=8 SLEs in 3 slice cultures). Although the magnitude of this relative change in chloride is uncorrelated to SLE onset time (n=8, p=0.31), we hypothesize that the pre-ictal burst-evoked chloride transients effectively decrease inhibition, leaving the network in a state of elevated excitability. We suspect that the timing of SLE onset may depend on the timing of activity, subsequent to the pre-ictal burst, in both principal neurons and interneurons.

Short duration events (<20s) in control conditions or in GABAzine produced chloride increases of 4.87±0.38 (mean±SEM, n=4 slice cultures, 52 events) and 2.97±0.07mM (mean ±SEM, n=4 slice cultures, 185 events) respectively (Figure 4A,B). To verify that these results were not specific to chronically epileptic organotypic slice cultures, Clomeleon results were confirmed in acute slices treated with both 4-AP and low-magnesium ACSF. In these recordings, ictal chloride transients recorded from the entorhinal cortex were 10.22±2.33mM (mean±SEM, n=5 SLEs in 2 slices from 2 animals). As in organotypic slice cultures, SLEs were blocked with the addition of 10μM GABAzine (Figure 3C,D).

To test whether observed changes in Clomeleon ratio could be explained by SLE-induced changes in pH, we imaged pyramidal cells during seizure activity in SNARF-1-AM-stained hippocampal slice cultures (Figure 5, largest recorded pH transient shown). During seizures, intracellular pH increased by an average of 0.080 ± 0.025 (mean±SEM, n=3 slices from two mice), corresponding to a ~4.8mM *decrease* in apparent chloride (Kuner and Augustine, 2000). Thus, the intracellular ictal chloride transients might actually be around 20% larger than those shown in Figures 3–4.

We hypothesized that the massive barrage of $GABA_A$ activation during the pre-ictal burst causes chloride to overwhelm KCC2 chloride transport capacity and accumulate to depolarizing concentrations, leaving the network in a hyper-excitable state. Chloride accumulation requires a sustained driving force for chloride entry, and thus only occurs when GABA currents cannot drive the membrane potential to the chloride equilibrium potential. This can occur as a consequence of depolarizing bicarbonate efflux through the $GABA_A$ ionophore (Bormann et al., 1987; Staley and Proctor, 1999), or as a consequence of concurrent activation of strongly depolarizing ligand and voltage-gated cationic conductances (Figure 1D; Doyon et al., 2011). Although it is not possible to block cationic conductances without fundamentally altering ictogenesis, the bicarbonate efflux is maintained by hydration of CO2, and so can be selectively diminished by inhibiting carbonic anhydrase (Staley et al., 1995). We therefore tested the effect of blocking the intracellular production of bicarbonate ions with the carbonic anhydrase inhibitor acetazolamide (ACTZ). As predicted, ACTZ statistically eliminated SLEs in 4-AP (n=8 slices from 5 animals, Figure 6). Thus, both enhancement of GABAergic inhibition via a non-chloride pathway (ACTZ) and blockade of GABAergic inhibition (GABAzine) eliminate seizures. Together these results support the hypothesis that activity-dependent

chloride accumulation and consequent shift in $GABA_A$ reversal potential contribute to a preictal decrease in inhibition.

Discussion

Epilepsy is often described in the context of an excitatory shift in the complex balance of inhibition and excitation in the brain, which can be caused by excessive neuronal sprouting (Cavazos et al., 1991; Sutula and Dudek, 2007), interneuron death (Maglóczky and Freund, 2005), ion channel mutations (Reid et al., 2009), pathological plasticity of synapses (Ben-Ari, 2008), or other causes. However, even an epileptic brain functions normally most of the time. The mechanisms underlying the sudden massive increase in neural activity during seizures remain elusive. In this paper, we provide evidence that ictal activity in GABAergic interneurons cause sufficient neuronal chloride accumulation that subsequent GABAergic activity will be depolarizing. In this mode, increased interneuron firing leads to increased principal cell activity, which in turn leads to more interneuron firing. This effective switch of interneurons from negative to positive feedback circuit elements contributed to seizure generation in both acute (4-AP) and chronic (organotypic) models of ictogenesis. This mechanism of transient positive feedback compliments previously described mechanisms such as extracellular K^+ accumulation (Fisher et al., 1976; Heinemann et al., 1977), and in fact because extracellular K+ accumulation alters the transport capacity of KCC2 (Staley and Proctor, 1999; Bihi et al., 2005) these two mechanisms of ictogenesis are likely to be complementary.

The question remains as to what drives interneuron firing during the pre-ictal burst. Recent evidence suggests that somatostatin-positive interneurons fire more readily than regular-spiking pyramidal cells or fast-spiking interneurons in response to activating stimuli such as extracellular current, low-Mg^{2+}/Ca^{2+} ACSF, mGluR agonists, and cholinergic agonists (Fanselow et al., 2008). Furthermore, somatostatin-positive interneurons have been shown to be coupled extensively via gap-junctions (Gibson et al., 1999; Fanselow et al., 2008; Amitai et al., 2002), which increases synchrony between coupled neurons (Fanselow et al., 2008). Our data are consistent with the hypothesis that interneurons such as the somatostatin-positive subtype activate most readily in response to the 4-AP-induced increase in excitability (Lopantsev and Avoli, 1998; Barbarosie et al., 2002). This activation could propagate throughout the gap-junction coupled network of interneurons to generate a synchronous event across the population of interneurons, corresponding to the interneuron-dominated pre-ictal burst observed in Figures 1–2. Alternatively, entorhinal cortical interneurons could be synchronized by long-range-projecting interneurons from the hippocampus (Melzer et al., 2012), a phenomenon recently shown to occur during pre-ictal activity in hippocamposeptal cells (Quilichini et al., 2012). Either method of synchronization would lead to a coordinated activation of post-synaptic $GABA_A$ receptors, which could explain the pre-ictal chloride accumulation observed in Figure 3.

The presence of GABA-mediated depolarizing potentials has been shown previously in the 4-AP model of seizure (Avoli et al., 1996). In those studies, depolarizing field potentials persisted even when blocking the NMDA and AMPA glutamate receptors, but they were prevented by $GABA_A$ antagonist bicuculline methiodide and μ-opiod agonist DAGO, which hyperpolarizes interneurons, reducing GABA release (Lupica and Dunwiddie, 1991). The GABA-mediated potentials were largest at the onset of ictal-like events, suggesting a potential role in ictogenesis. The large GABA conductance induces an activity-dependent neuronal chloride accumulation and a consequent depolarizing shift in the $GABA_A$ reversal potential. The chloride accumulation is most pronounced in structures with large numbers of receptors per unit volume, e.g. dendrites, and less pronounced at the soma (Staley and Proctor, 1999; Isomura et al., 2003; Doyon et al., 2011). An open question has been whether

somatic chloride accumulation is sufficient to induce GABA-mediated excitation, or whether this effect would be limited to dendrites, and, perhaps due to ClC-2 chloride regulation (Foldy et al., 2010), shunted at the soma by depolarizing but still inhibitory GABAergic conductances. Using the Nernst equation, we calculated the somatic chloride accumulations observed here to correspond to 26±3mV (mean±SEM) shifts in E_{GABA} (to levels positive to action potential threshold). This shift in E_{GABA} at the soma supports the idea that ictal activity causes GABA to become frankly excitatory.

We provide direct evidence of the interneuron-dominated pre-ictal burst, presumably responsible for GABA-mediated potentials. Our data suggest that GABA-mediated activity at ictogenesis floods postsynaptic targets with chloride, resulting in an ineffective inhibitory network that contributes to the generation of a seizure. These data are consistent with recent findings of preictal spikes that elicit synaptic activity with dramatically shifted reversal potentials in pyramidal neurons in both intact mouse hippocampal preparations (Zhang et al., 2012) and resected human epileptic brain tissue (Huberfeld et al., 2007, 2011). Our data contribute to the study of complex pre-ictal network phenomena by providing a large simultaneous sampling of calcium or chloride concentrations in interneurons and principal cells. These data and the robust effect of carbonic anhydrase blockade favor GABAergic over glutamatergic activity as the mechanism underlying the sharp pre-ictal shift in the reversal potential of postsynaptic potentials in pyramidal cells. Future studies employing additional interneuron labeling, voltage-dependent fluorophores, and additional models of epilepsy will further clarify the critical mechanisms of preictal loss of inhibition.

Studying the role of GABAergic inhibition in epilepsy is complicated by both the wide distribution of intracellular chloride concentrations (Glykys et al., 2009) and the highly variable expression of KCC2 (Huberfeld et al., 2007). This variability makes it difficult to predict what the net effect of blocking GABA synapses will be. In organotypic slices cut from different planes (but otherwise similarly prepared), GABA blockade has been shown to have opposite effects on network excitability (McBain et al., 1989, Figures 3–4). In recordings from human tissue, IPSP reversal potentials varied from hyperpolarizing to depolarizing depending on KCC2 expression (Huberfeld et al., 2007). Likely, the overall role of GABA in the network depends on the distribution of intracellular chloride, chloride transporter expression, and interneuron connectivity. Our data elucidate another degree of freedom for GABA in which the net effect of GABA may be inhibitory at rest, but becomes transiently excitatory during ictogenesis. We hypothesize that epilepsy can develop in part from pathologies that make chloride gradients at $GABA_A$ synapses labile such as enhanced functional inhibition. These include increased GABA synapse activity, (Buckmaster and Dudek, 1997), reduced expression of KCC2 and consequent reduced chloride efflux, (Jin et al., 2005; de Guzman et al., 2006; Pathak et al., 2007), and increased $GABA_A$ synaptic density (Bausch, 2005; Thind et al., 2010) with increased postsynaptic chloride influx.

Supplementary Material

Refer to Web version on PubMed Central for supplementary material.

Acknowledgments

This work was supported by grants from the NIH, the Epilepsy Foundation and the Burroughs Wellcome Fund. We thank G. Feng, T. Kuner, and G.J. Augustine for generously providing us with the Clomeleon mice.

References

Amitai Y, Gibson JR, Beierlein M, Patrick SL, Ho AM, Connors BW, Golomb D. The Spatial Dimensions of Electrically Coupled Networks of Interneurons in the Neocortex. J Neurosci. 2002; 22:4142–4152. [PubMed: 12019332]

Aronica E, Boer K, Redeker S, Spliet WGM, van Rijen PC, Troost D, Gorter JA. Differential expression patterns of chloride transporters, Na+-K+-2Cl−-cotransporter and K+-Cl−-cotransporter, in epilepsy-associated malformations of cortical development. Neuroscience. 2007; 145:185–196. [PubMed: 17207578]

Avoli M, Barbarosie M, Lucke A, Nagao T, Lopantsev V, Kohling R. Synchronous GABA-Mediated Potentials and Epileptiform Discharges in the Rat Limbic System In Vitro. J Neurosci. 1996; 16:3912–3924. [PubMed: 8656285]

Barbarosie M, Avoli M. CA3-Driven Hippocampal-Entorhinal Loop Controls Rather than Sustains In Vitro Limbic Seizures. J Neurosci. 1997; 17:9308–9314. [PubMed: 9364076]

Barbarosie M, Louvel J, D'Antuono M, Kurcewicz I, Avoli M. Masking synchronous GABA-mediated potentials controls limbic seizures. Epilepsia. 2002; 43:1469–1479. [PubMed: 12460247]

Bausch SB. Axonal sprouting of GABAergic interneurons in temporal lobe epilepsy. Epilepsy Behav. 2005; 7:390–400. [PubMed: 16198153]

Ben-Ari Y. Epilepsies and neuronal plasticity: for better or for worse? Dialogues Clin Neurosci. 2008; 10:17–27. [PubMed: 18472481]

Ben-Ari Y, Holmes GL. The multiple facets of gamma-aminobutyric acid dysfunction in epilepsy. Curr Opin Neurol. 2005; 18:141–145. [PubMed: 15791144]

Berdichevsky Y, Sabolek H, Levine JB, Staley KJ, Yarmush ML. Microfluidics and multielectrode array-compatible organotypic slice culture method. J Neurosci Methods. 2009; 178:59–64. [PubMed: 19100768]

Berglund K, Schleich W, Krieger P, Loo LS, Wang D, Cant NB, Feng G, Augustine GJ, Kuner T. Imaging synaptic inhibition in transgenic mice expressing the chloride indicator, Clomeleon. Brain Cell Biol. 2006; 35:207–228. [PubMed: 18398684]

Bihi RI, Jefferys JGR, Vreugdenhil M. The role of extracellular potassium in the epileptogenic transformation of recurrent GABAergic inhibition. Epilepsia. 2005; 46(Suppl 5):64–71. [PubMed: 15987256]

Bormann J, Hamill OP, Sakmann B. Mechanism of anion permeation through channels gated by glycine and gamma-aminobutyric acid in mouse cultured spinal neurones. J Physiol. 1987; 385:243–286. [PubMed: 2443667]

Buckmaster PS, Dudek FE. Neuron loss, granule cell axon reorganization, and functional changes in the dentate gyrus of epileptic kainate-treated rats. J Comp Neurol. 1997; 385:385–404. [PubMed: 9300766]

Cavazos JE, Golarai G, Sutula TP. Mossy fiber synaptic reorganization induced by kindling: time course of development, progression, and permanence. J Neurosci. 1991; 11:2795–2803. [PubMed: 1880549]

Dallwig R, Deitmer JW, Backus KH. On the mechanism of GABA-induced currents in cultured rat cortical neurons. Pflugers Arch. 1999; 437:289–297. [PubMed: 9929572]

Doyon N, Prescott S, Castonguay A, Godin A, De Koninck Y. Efficacy of synaptic inhibition depends on multiple, dynamically interacting mechanisms implicated in chloride homeostasis. PLoS Computational Biology. 2011 In press.

Dyhrfjeld-Johnsen J, Berdichevsky Y, Swiercz W, Sabolek H, Staley KJ. Interictal spikes precede ictal discharges in an organotypic hippocampal slice culture model of epileptogenesis. J Clin Neurophysiol. 2010; 27:418–424. [PubMed: 21076333]

Fanselow EE, Richardson KA, Connors BW. Selective, State-Dependent Activation of Somatostatin-Expressing Inhibitory Interneurons in Mouse Neocortex. J Neurophysiol. 2008; 100:2640–2652. [PubMed: 18799598]

Fisher RS, Pedley TA, Moody WJ Jr, Prince DA. The role of extracellular potassium in hippocampal epilepsy. Arch Neurol. 1976; 33:76–83. [PubMed: 1252153]

Foldy C, Lee S-H, Morgan RJ, Soltesz I. Regulation of fast-spiking basket cell synapses by the chloride channel ClC-2. Nat Neurosci. 2010; 13:1047–1049. [PubMed: 20676104]

Fujiwara-Tsukamoto Y, Isomura Y, Kaneda K, Takada M. Synaptic interactions between pyramidal cells and interneurone subtypes during seizure-like activity in the rat hippocampus. J Physiol. 2004; 557:961–979. [PubMed: 15107470]

Gähwiler BH. Organotypic monolayer cultures of nervous tissue. J Neurosci Methods. 1981; 4:329–342. [PubMed: 7033675]

Gibson JR, Beierlein M, Connors BW. Two networks of electrically coupled inhibitory neurons in neocortex. Nature. 1999; 402:75–79. [PubMed: 10573419]

Glykys J, Dzhala VI, Kuchibhotla KV, Feng G, Kuner T, Augustine G, Bacskai BJ, Staley KJ. Differences in Cortical versus Subcortical GABAergic Signaling: A Candidate Mechanism of Electroclinical Uncoupling of Neonatal Seizures. Neuron. 2009; 63:657–672. [PubMed: 19755108]

de Guzman P, Inaba Y, Biagini G, Baldelli E, Mollinari C, Merlo D, Avoli M. Subiculum network excitability is increased in a rodent model of temporal lobe epilepsy. Hippocampus. 2006; 16:843–860. [PubMed: 16897722]

Heinemann U, Lux HD, Gutnick MJ. Extracellular free calcium and potassium during paroxsmal activity in the cerebral cortex of the cat. Exp Brain Res. 1977; 27:237–243. [PubMed: 880984]

Huberfeld G, Menendez de la Prida L, Pallud J, Cohen I, Le Van Quyen M, Adam C, Clemenceau S, Baulac M, Miles R. Glutamatergic pre-ictal discharges emerge at the transition to seizure in human epilepsy. Nat Neurosci. 2011; 14:627–634. [PubMed: 21460834]

Huberfeld G, Wittner L, Clemenceau S, Baulac M, Kaila K, Miles R, Rivera C. Perturbed chloride homeostasis and GABAergic signaling in human temporal lobe epilepsy. J Neurosci. 2007; 27:9866–9873. [PubMed: 17855601]

Isomura Y, Sugimoto M, Fujiwara-Tsukamoto Y, Yamamoto-Muraki S, Yamada J, Fukuda A. Synaptically Activated Cl− Accumulation Responsible for Depolarizing GABAergic Responses in Mature Hippocampal Neurons. Journal of Neurophysiology. 2003; 90:2752–2756. [PubMed: 14534278]

Jin X, Huguenard JR, Prince DA. Impaired Cl− extrusion in layer V pyramidal neurons of chronically injured epileptogenic neocortex. J Neurophysiol. 2005; 93:2117–2126. [PubMed: 15774713]

Köhling R, Vreugdenhil M, Bracci E, Jefferys JG. Ictal epileptiform activity is facilitated by hippocampal GABAA receptor-mediated oscillations. J Neurosci. 2000; 20:6820–6829. [PubMed: 10995826]

Kosobud AE, Crabbe JC. Genetic correlations among inbred strain sensitivities to convulsions induced by 9 convulsant drugs. Brain Research. 1990; 526:8–16. [PubMed: 2078820]

Kumar SS, Buckmaster PS. Hyperexcitability, Interneurons, and Loss of GABAergic Synapses in Entorhinal Cortex in a Model of Temporal Lobe Epilepsy. The Journal of Neuroscience. 2006; 26:4613–4623. [PubMed: 16641241]

Kuner T, Augustine GJ. A Genetically Encoded Ratiometric Indicator for Chloride: Capturing Chloride Transients in Cultured Hippocampal Neurons. Neuron. 2000; 27:447–459. [PubMed: 11055428]

de Lanerolle NC, Kim JH, Robbins RJ, Spencer DD. Hippocampal interneuron loss and plasticity in human temporal lobe epilepsy. Brain Res. 1989; 495:387–395. [PubMed: 2569920]

Lee HHC, Deeb TZ, Walker JA, Davies PA, Moss SJ. NMDA receptor activity downregulates KCC2 resulting in depolarizing GABAA receptor-mediated currents. Nat Neurosci. 2011; 14:736–743. [PubMed: 21532577]

Lillis KP, Eng A, White JA, Mertz J. Two-photon imaging of spatially extended neuronal network dynamics with high temporal resolution. J Neurosci Methods. 2008; 172:178–184. [PubMed: 18539336]

Lopantsev V, Avoli M. Participation of GABAA-mediated inhibition in ictallike discharges in the rat entorhinal cortex. J Neurophysiol. 1998; 79:352–360. [PubMed: 9425204]

Lupica CR, Dunwiddie TV. Differential effects of mu- and delta-receptor selective opioid agonists on feedforward and feedback GABAergic inhibition in hippocampal brain slices. Synapse. 1991; 8:237–248. [PubMed: 1656539]

Maglóczky Z, Freund TF. Impaired and repaired inhibitory circuits in the epileptic human hippocampus. Trends in Neurosciences. 2005; 28:334–340. [PubMed: 15927690]

Marchionni I, Maccaferri G. Quantitative dynamics and spatial profile of perisomatic GABAergic input during epileptiform synchronization in the CA1 hippocampus. J Physiol (Lond). 2009; 587:5691–5708. [PubMed: 19840998]

Martin MS, Dutt K, Papale LA, Dubé CM, Dutton SB, de Haan G, Shankar A, Tufik S, Meisler MH, Baram TZ, Goldin AL, Escayg A. Altered function of the SCN1A voltage-gated sodium channel leads to gamma-aminobutyric acid-ergic (GABAergic) interneuron abnormalities. J Biol Chem. 2010; 285:9823–9834. [PubMed: 20100831]

McBain CJ, Boden P, Hill RG. Rat hippocampal slices “in vitro” display spontaneous epileptiform activity following long-term organotypic culture. J Neurosci Methods. 1989; 27:35–49. [PubMed: 2563782]

Melzer S, Michael M, Caputi A, Eliava M, Fuchs EC, Whittington MA, Monyer H. Long-Range–Projecting GABAergic Neurons Modulate Inhibition in Hippocampus and Entorhinal Cortex. Science. 2012; 335:1506–1510. [PubMed: 22442486]

Netoff TI, Banks MI, Dorval AD, Acker CD, Haas JS, Kopell N, White JA. Synchronization in hybrid neuronal networks of the hippocampal formation. J Neurophysiol. 2005; 93:1197–1208. [PubMed: 15525802]

Oliva AA, Jiang M, Lam T, Smith KL, Swann JW. Novel hippocampal interneuronal subtypes identified using transgenic mice that express green fluorescent protein in GABAergic interneurons. J Neurosci. 2000; 20:3354–3368. [PubMed: 10777798]

Pathak HR, Weissinger F, Terunuma M, Carlson GC, Hsu F-C, Moss SJ, Coulter DA. Disrupted dentate granule cell chloride regulation enhances synaptic excitability during development of temporal lobe epilepsy. J Neurosci. 2007; 27:14012–14022. [PubMed: 18094240]

Quilichini PP, Le Van Quyen M, Ivanov A, Turner DA, Carabalona A, Gozlan H, Esclapez M, Bernard C. Hub GABA Neurons Mediate Gamma-Frequency Oscillations at Ictal-like Event Onset in the Immature Hippocampus. Neuron. 2012; 74:57–64. [PubMed: 22500630]

Reid CA, Berkovic SF, Petrou S. Mechanisms of human inherited epilepsies. Prog Neurobiol. 2009; 87:41–57. [PubMed: 18952142]

Sheldon C, Cheng YM, Church J. Concurrent measurements of the free cytosolic concentrations of H+ and Na+ ions with fluorescent indicators. Pflugers Arch. 2004; 449:307–318. [PubMed: 15452716]

Shimizu-Okabe C, Tanaka M, Matsuda K, Mihara T, Okabe A, Sato K, Inoue Y, Fujiwara T, Yagi K, Fukuda A. KCC2 was downregulated in small neurons localized in epileptogenic human focal cortical dysplasia. Epilepsy Research. 2011; 93:177–184. [PubMed: 21256718]

Staley KJ, Proctor WR. Modulation of mammalian dendritic GABA(A) receptor function by the kinetics of Cl− and HCO3− transport. J Physiol (Lond). 1999; 519(Pt 3):693–712. [PubMed: 10457084]

Staley KJ, Soldo BL, Proctor WR. Ionic mechanisms of neuronal excitation by inhibitory GABAA receptors. Science. 1995; 269:977–981. [PubMed: 7638623]

Sutula TP, Dudek FE. Unmasking recurrent excitation generated by mossy fiber sprouting in the epileptic dentate gyrus: an emergent property of a complex system. Prog Brain Res. 2007; 163:541–563. [PubMed: 17765737]

Taira T, Lamsa K, Kaila K. Posttetanic excitation mediated by GABA(A) receptors in rat CA1 pyramidal neurons. J Neurophysiol. 1997; 77:2213–2218. [PubMed: 9114269]

Thind KK, Yamawaki R, Phanwar I, Zhang G, Wen X, Buckmaster PS. Initial loss but later excess of GABAergic synapses with dentate granule cells in a rat model of temporal lobe epilepsy. J Comp Neurol. 2010; 518:647–667. [PubMed: 20034063]

Xu C, Zipfel W, Shear JB, Williams RM, Webb WW. Multiphoton fluorescence excitation: new spectral windows for biological nonlinear microscopy. Proc Natl Acad Sci USA. 1996; 93:10763–10768. [PubMed: 8855254]

Zhang ZJ, Koifman J, Shin DS, Ye H, Florez CM, Zhang L, Valiante TA, Carlen PL. Transition to Seizure: Ictal Discharge Is Preceded by Exhausted Presynaptic GABA Release in the Hippocampal CA3 Region. J Neurosci. 2012; 32:2499–2512. [PubMed: 22396423]

Ziburkus J, Cressman JR, Barreto E, Schiff SJ. Interneuron and pyramidal cell interplay during in vitro seizure-like events. J Neurophysiol. 2006; 95:3948–3954. [PubMed: 16554499]

Highlights

- Seizures *in vitro* are preceded by an interneuron-dominated preictal burst.
- Interneuron-pyramidal cell firing is tightly coupled following the preictal burst.
- Chloride transiently increases during seizure, raising EGABA above spike threshold.
- Blocking GABAA receptors results in short bursting, small chloride transients.

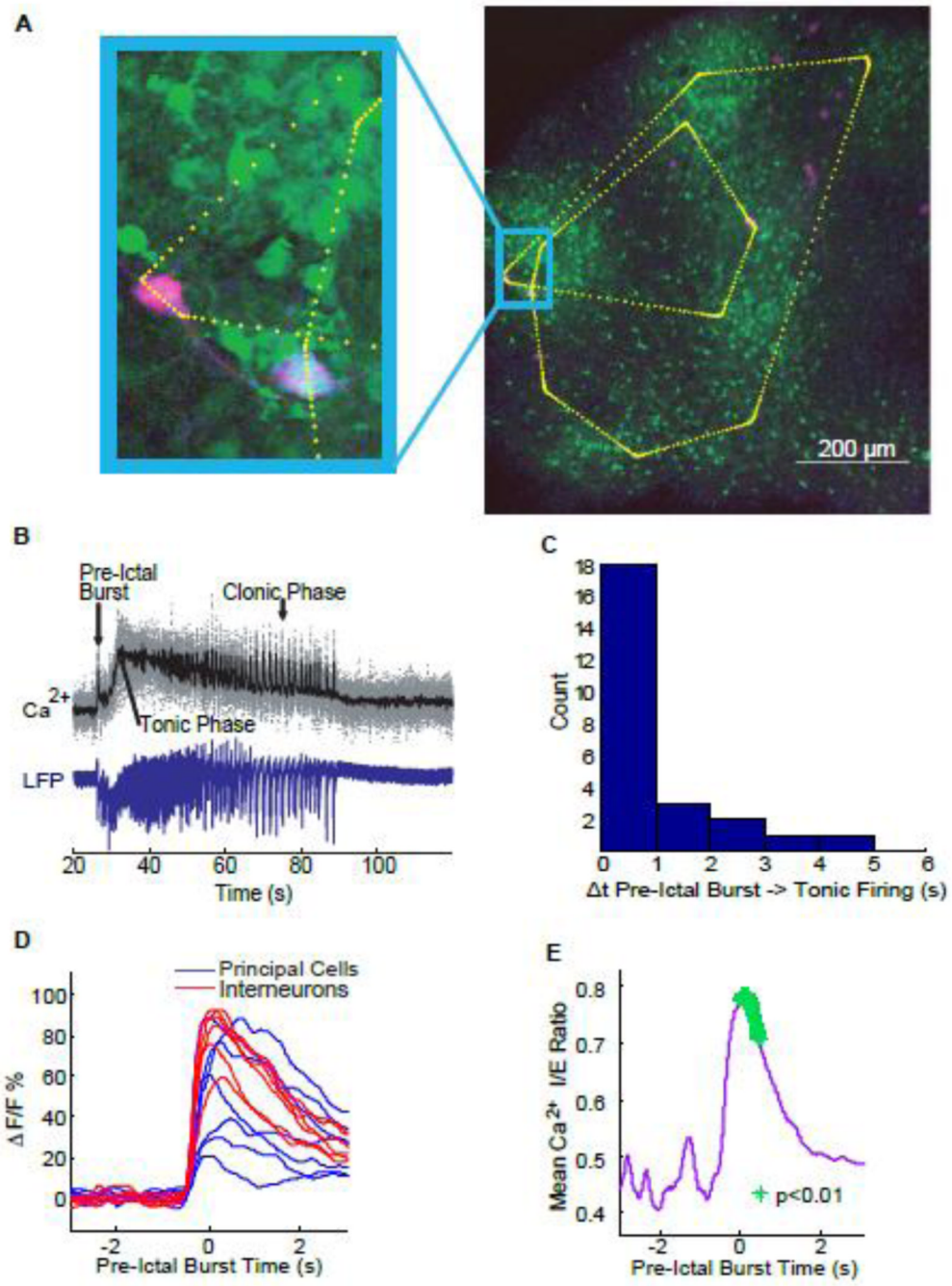

Figure 1. Targeted Path Scanning of interneurons and principle cells

A) Using two-photon TPS, a laser path (yellow dotted line) is selected that includes cells stained with Indo-1 only (principal cells, green) and cells that express GFP and are stained with Indo-1 (interneurons, pink). B) 50 µM 4-AP ACSF produces SLEs that have a characteristic pattern (mean calcium: black, LFP: blue) beginning with a pre-ictal burst, followed by the tonic phase of the SLE, and finishing with clonic discharges. C) The delay between the pre-ictal burst and the onset of the tonic phase of the SLE varied within a range of 0–5s. D) A sample of 7 interneuron (red) and 7 principal cell (blue) calcium traces from a single pre-ictal burst (at t=0) in a single slice suggests that calcium transients are larger in interneurons. E) Indeed pooling calcium data across all recorded pre-ictal bursts (n=22

SLEs, 533 principal cells, 115 interneurons) reveals a significant shift in the balance of interneuron vs. principal cell calcium concentration ($p<0.01$, green asterisks indicate time points at which I-E ratio is significantly different from baseline).

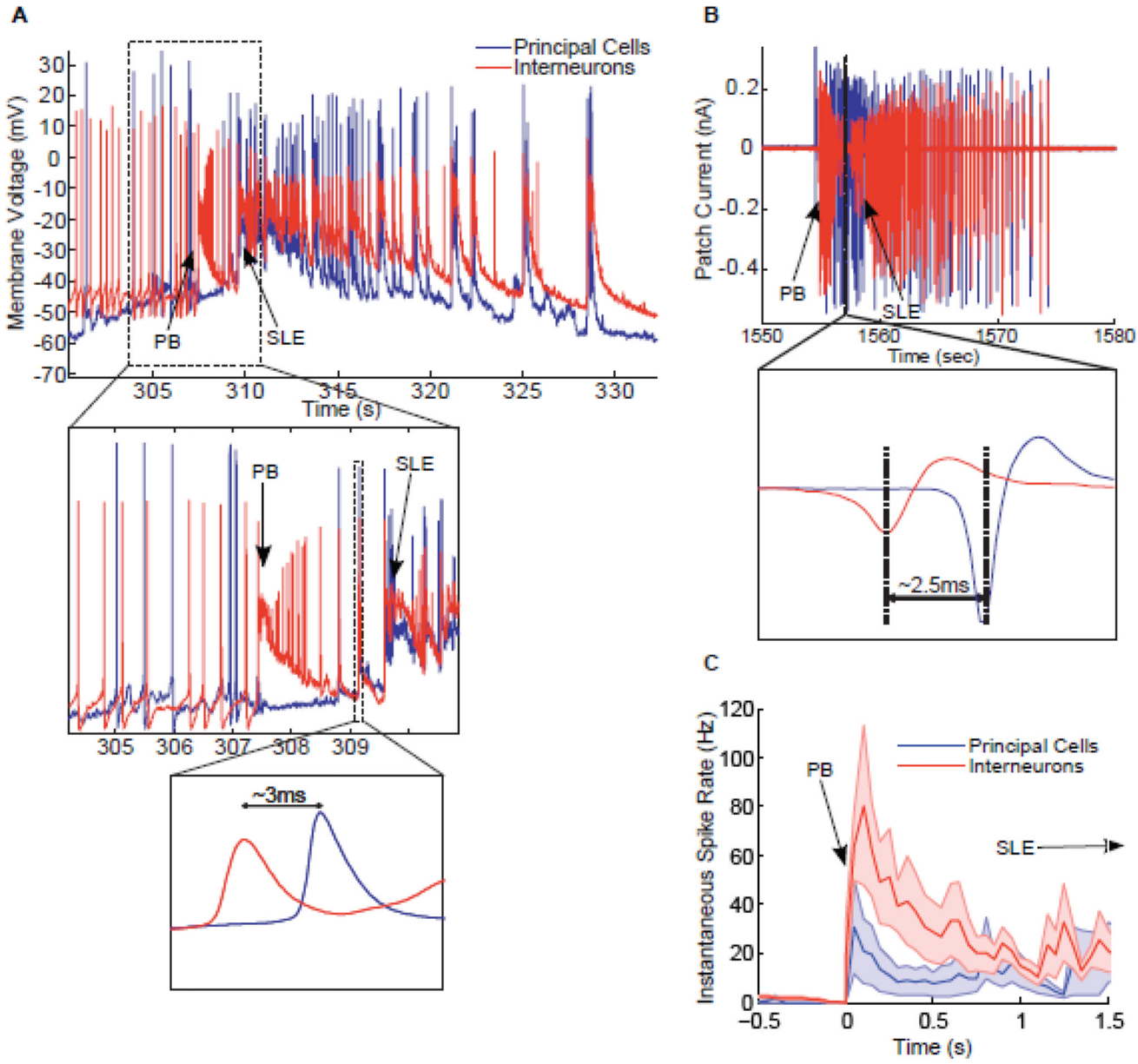

Figure 2. Interneurons fire at higher rates than principal cells at ictogenesis

Using both whole-cell and loose-patch clamp recordings (A and B, respectively), we observed (insets) uncorrelated interneuron (red) and principal cell (blue) firing before SLE onset and precise I-before-E firing immediately following the interneuron dominated pre-ictal burst (PB). C) Instantaneous spike rates calculated at the time of the pre-ictal burst (t=0 is time of pre-ictal burst onset, shaded regions include mean ± SEM) further validate that the elevated interneuron calcium levels observed in Figure 1 are a result of an increase in interneuron firing rate.

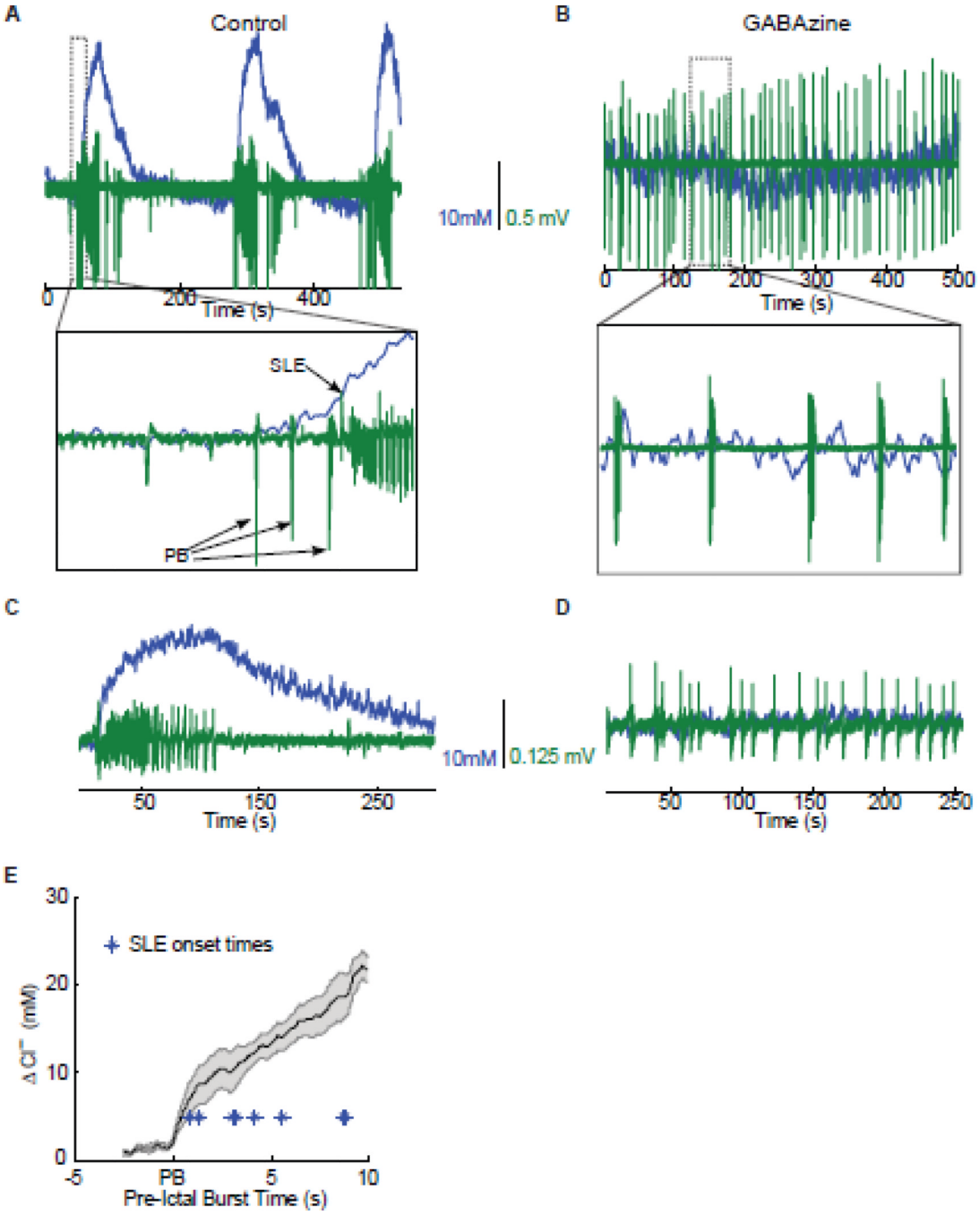

Figure 3. Intracellular chloride is elevated during ictogenesis

A) At SLE onset there was a sharp decrease in clomeleon ratio (YFP/CFP), corresponding to an increase in intracellular chloride. B) Blocking $GABA_A$ with 10uM GABAzine eliminated SLEs and the corresponding high-amplitude chloride transients, leaving interictal-like discharges at a rate of ~0.1Hz. C,D) Acute slices treated with 4-AP and zero-Mg^{2+} ACSF produced similar results to those observed in A,B, indicating that the effect is not specific to chronically epileptic tissue. E) Aligning chloride measurements at the time of the pre-ictal bursts reveals a pre-ictal burst-evoked increase in intracellular chloride. The mean chloride concentration at the time of SLE onset (indicated by * for each of the 8 SLEs) was

6.27±1.23mM above baseline. A,B, and insets share a scale bar. C and D also share a scalebar.

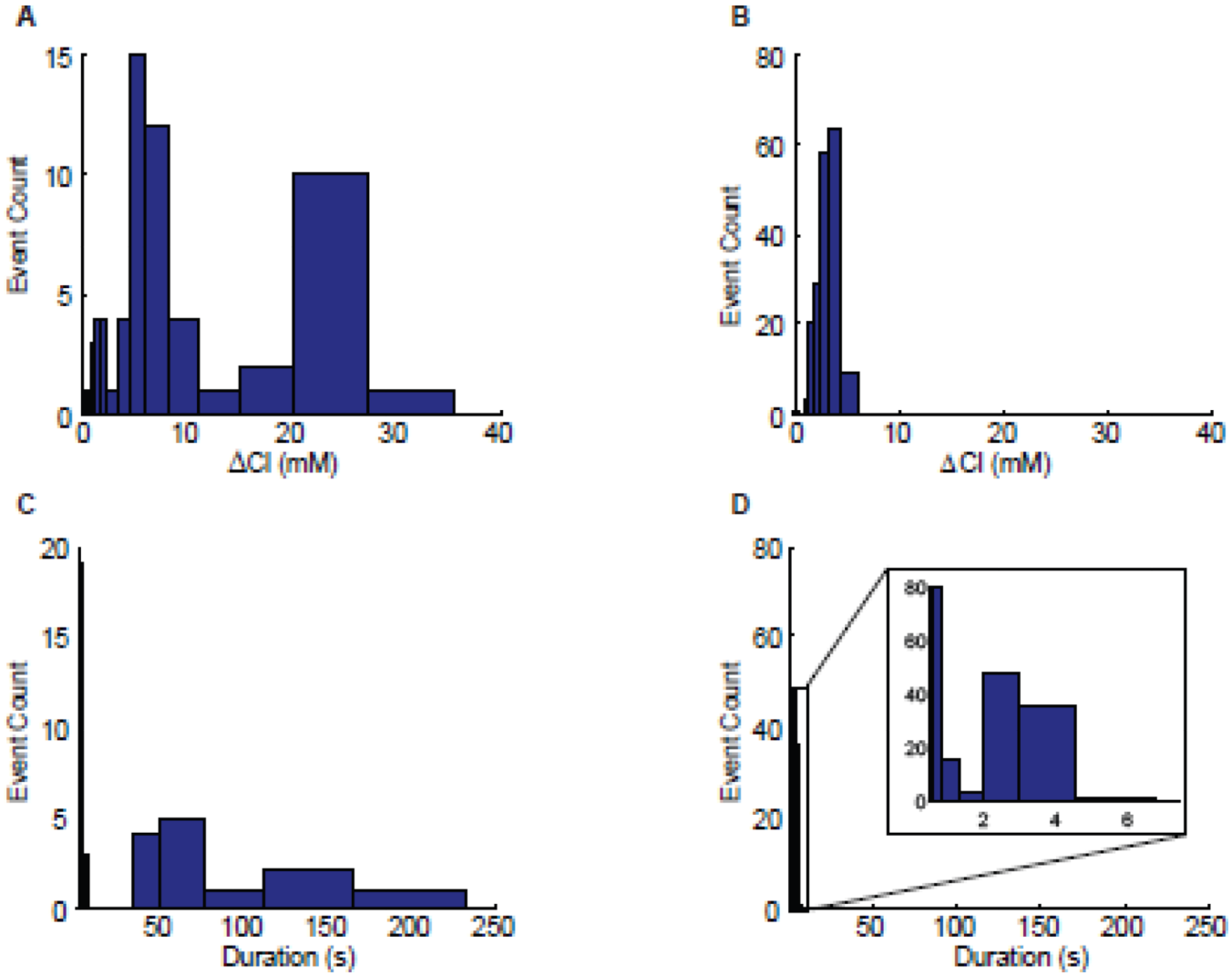

Figure 4. GABA becomes depolarizing during seizure, is necessary for ictogenesis

A) During SLE, chloride increased by 22.95±0.73mM, corresponding to a calculated 26±3mV depolarization of the $GABA_A$ receptor reversal potential. B) $GABA_A$ blockade eliminated SLEs, leaving burst-evoked chloride peaks of 2.97±0.07mM. C) Under control conditions, organotypic slices produced bouts of electrical activity of short duration, corresponding to interictal bursting and of long duration, corresponding to SLEs, while D) GABAzine eliminated prolonged SLEs, leaving behind only short duration events. Log-spaced bins (but not axes) were used for these histograms to highlight the mixture of many short-duration events and occasional long-duration events.

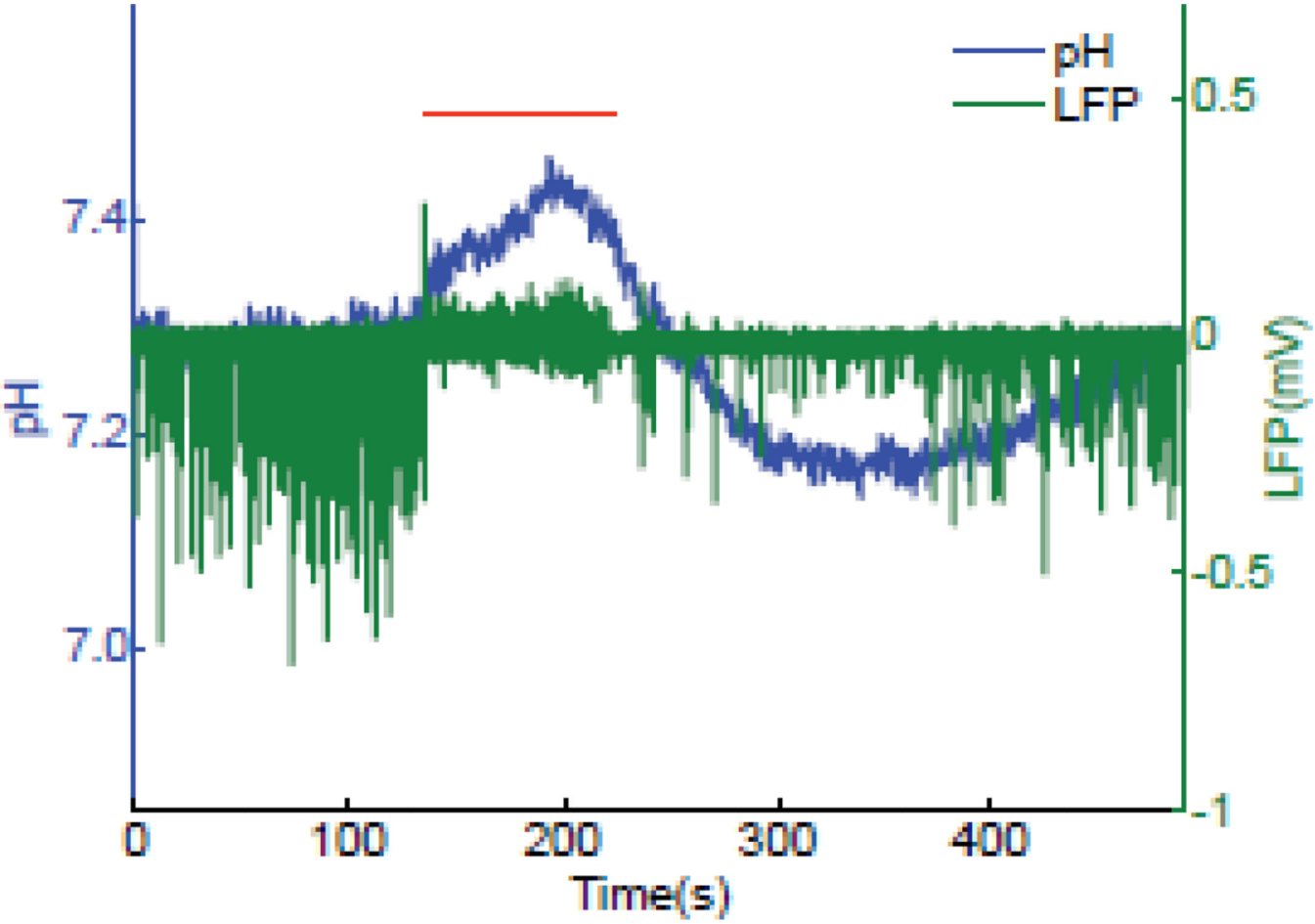

Figure 5. Ictal pH changes

Organotypic slices prepared from wild-type mice were stained with the ratiometric pH indicator SNARF-1 AM. Spontaneous SLEs were apparent (red bar) in a synchronously recorded field potential (green). Both the polarity (alkali ictal transient) and low amplitude (0.080 ± 0.025, mean±SEM, n=3 slices) of observed pH changes (blue) were insufficient to account for changes observed in intracellular chloride using Clomeleon.

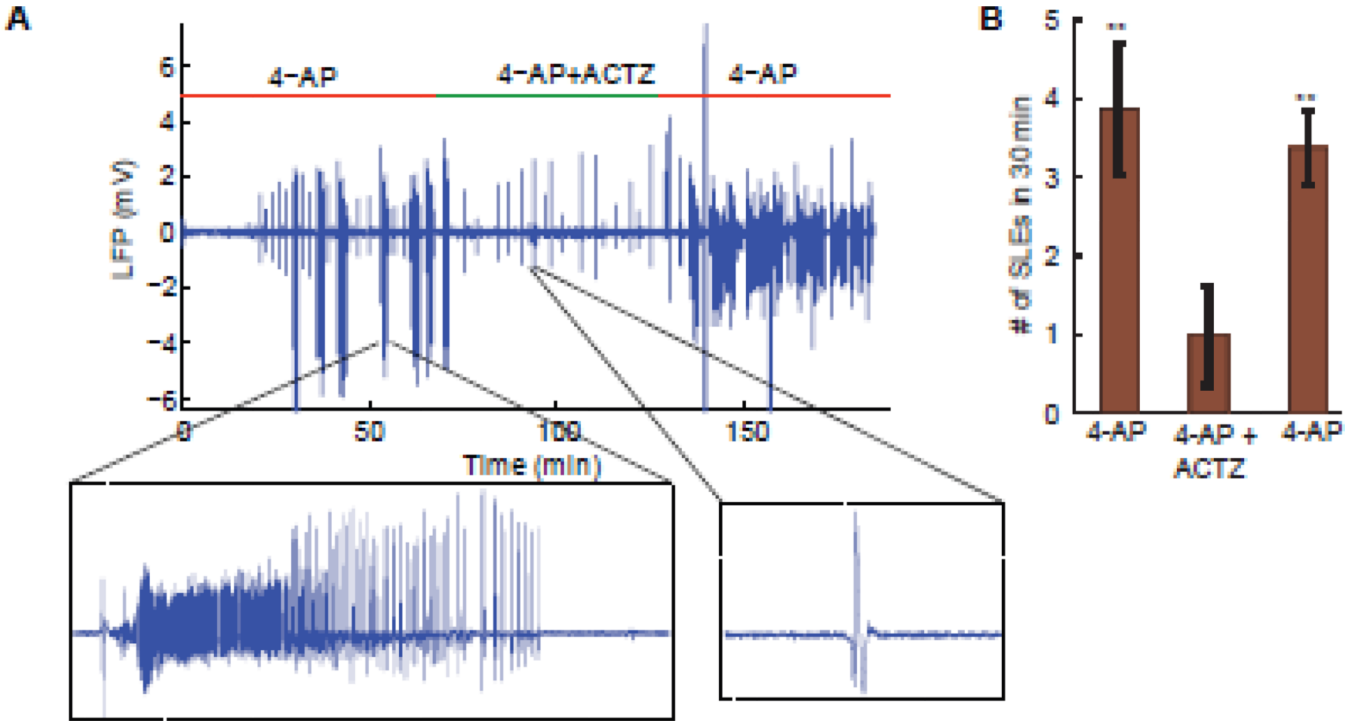

Figure 6. Bicarbonate current contributes to ictogenesis

A) In 4-AP-treated acute slices from GIN mice, pharmacologically hyperpolarizing the $GABA_A$ reversal potential by blocking intracellular bicarbonate production with acetazolamide (ACTZ) eliminates SLEs, leaving only interictal bursts. Upon washout of ACTZ, SLEs return. B) ACTZ reversibly eliminates SLEs in 4-AP (n = 11, ** indicate that the number of SLEs is significantly different from zero, $p<0.05$).